Multi-band model Hamiltonian for tunnel devices with van der Waals heterojunctions

Owen Loison
Université Paris-Saclay, CNRS
Centre de Nanosciences et de Nanotechnologies
91120, Palaiseau, France
owen.loison@universite-paris-saclay.fr

Adel M'Foukh
Université Paris-Saclay, CNRS
Centre de Nanosciences et de Nanotechnologies
91120, Palaiseau, France
adel.mfoukh@cnrs.fr

Davide Romanin
Université Paris-Saclay, CNRS
Centre de Nanosciences et de Nanotechnologies
91120, Palaiseau, France
davide.romanin@cnrs.fr

Marco Pala
DPIA
University of Udine
Udine, Italy
marco.pala@uniud.it

Philippe Dollfus
CNRS, Université Paris-Saclay
Centre de Nanosciences et de Nanotechnologies
91120, Palaiseau, France
philippe.dollfus@cnrs.fr

***Abstract*—We study the electronic properties of a van der Waals (vdW) heterostructure made of $SnSe_2$ and WSe_2 by *ab-initio* methods in order to simulate an Esaki diode built with these materials. We use Density Functional Theory (DFT) to parametrize a $\mathbf{k}\cdot\mathbf{p}$ model in order to achieve the transport calculations. Furthermore we introduce a tunneling coefficient parametrized by DFT. This coefficient depends on the electric field in the device in order to precisely describe the quantum tunneling happening in the heterostructure. This model Hamiltonian is then used to compute current-voltage characteristics for our Esaki diode via Non-Equilibrium Green's Functions (NEGF) calculations.**

***Index Terms*—quantum transport, NEGF, 2D materials, broken gap.**

I. Introduction

Among numerous possibilities for adjusting the electronic properties of 2D materials, vdW heterostructures of Transition Metal Dichalcogenides (TMDs) may provide staggered and broken-gap heterojunctions that can enhance on-state currents of tunnel devices [1] [2]. The use of *ab initio* Hamiltonians to simulate the transport properties of these systems can be challenging in the case of supercells with a large number of atoms arising either from lattice mismatch or from arbitrary orientation of the two lattices. In this work, we propose a model Hamiltonian based on a multiband envelope function model calibrated against DFT and apply it to an Esaki diode [3] based on a vertical $SnSe_2$/WSe_2 heterostructure. Due to the importance of vertical tunneling between the two materials, we propose a field-dependent expression for the tunneling coupling, which can be assessed with DFT simulations.

II. Transport model

To compute the electronic properties of this heterostructure, we used a plane-wave DFT approach, as implemented in Quantum ESPRESSO [4], with Perdew-Burke-Ernzerhof [5] functionals, a $6 \times 6 \times 1$ Monkhorst-Pack grid of k-points and spin-orbit taken into account. Van der Waals correction were considered in the calculations with Grimme-D3 [6]. The unit cell of each isolated material has been relaxed and resulted in a lattice parameter of 3.32 Å for monolayer WSe_2 and 3.86 Å for monolayer $SnSe_2$. We created a common supercell of 6.66 Å from a 2×2 cell of WSe_2 and a $\sqrt{3}\times\sqrt{3}$ cell of $SnSe_2$, adding up to a 21 atom supercell and causing a stress of less than 1% for both materials. In Fig. 1 we plot the band structure of this system, exhibiting a broken gap configuration with the top of the valence band (VB) (made of WSe_2 states) being above the bottom of the conduction band (CB) (made of $SnSe_2$ states). The broken gap value is about 0.013 eV.

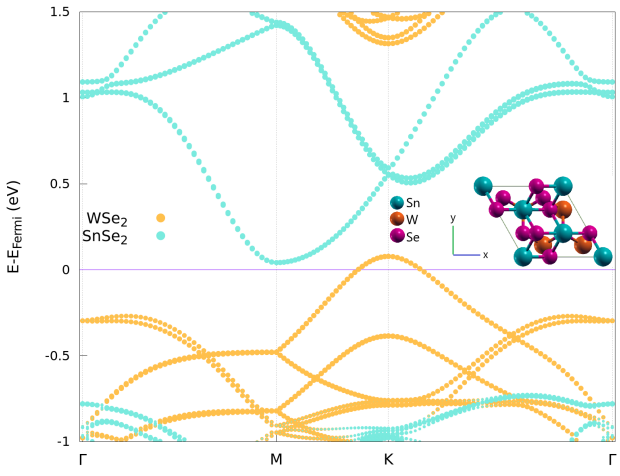

Fig. 1. Electronic band structure of the $SnSe_2$/WSe_2 heterostructure projected over the states of $SnSe_2$ (light blue) and WSe_2 (orange). In the inset, we show the stick-and-ball model of the $SnSe_2$/WSe_2 heterostructure, where green, magenta and orange balls are the Sn, W and Se atoms respectively.

The model Hamiltonian we used for transport calculations is based on the envelope function method proposed by Ref. [7]. We simplified the problem by assuming that the only relevant coupling is due to the vertical tunneling between the minimum

of the CB of $SnSe_2$ and the maximum of the VB of WSe_2. This model can be naturally extended to any heterostructure where other bands become relevant to electron transport or other types of couplings become important.

In our simple case, the Schrödinger problem can then be described by a 2×2 Hamiltonian matrix:

$$H = \begin{pmatrix} H_1(x, z_t) & H_T(x) \\ H_T^*(x) & H_2(x, z_b) \end{pmatrix}$$
$$\begin{cases} H_1(x, z_t) = -\dfrac{\hbar^2}{2m_{cx}}\nabla_x^2 + \dfrac{\hbar^2}{2m_{cy}}k_y^2 + E_0 + U(x, z_t) \\ H_2(x, z_b) = \dfrac{\hbar^2}{2m_{vx}}\nabla_x^2 - \dfrac{\hbar^2}{2m_{vy}}(k_y - \Delta k_y)^2 + U(x, z_b) \end{cases} \tag{1}$$

where $m_{cx,cy,vx,vy} = (0.202, 0.427, 0.342, 0.342) \times m_0$ are effective masses, $\Delta k_y = 3.15\,\mathrm{nm}^{-1}$ is the lateral momentum mismatch [8], E_0 the band offset between the two materials, $U(x, z)$ the potential energy, and we have assumed the system to be periodic along the lateral direction (y-axis) and that the direction of transport is on the x-axis. The band-to-band tunneling coefficient can be estimated as

$$H_T(x) = -\frac{i\hbar}{m_0}\frac{U(x, z_t) - U(x, z_b)}{z_t - z_b}\frac{p_{c,v}}{E_c - E_v} \tag{2}$$

where $z_{t,b}$ are the vertical positions of the top layer $SnSe_2$ and bottom layer WSe_2, respectively, and the momentum matrix element

$$p_{c,v} = -i\hbar \int_{\text{u.c.}} d\mathbf{r}\, u_c(\mathbf{r})\nabla_z u_v(\mathbf{r}) \tag{3}$$

which we evaluated using DFT and resulted to be $3.98 \times 10^{-2}\,\mathrm{eV} \cdot \text{Å}$.

To validate the model, we computed the distance between the CB minimum and the VB maximum with the field-dependent expression derived from the effective Hamiltonian and plot the field-dependent curve in Fig. 2. Using Quantum ESPRESSO [9], we were able to add a gate inside our cell and simulate how the electronic properties evolve with the electric field created by the external gate, thus measuring the band evolution with the vertical electric field and assessing the bandgap opening. This is shown in Fig. 2, where we measured the gap of the heterostructure for different gate voltages. As can be seen, our simplified model reproduces very well the electric-field dependence resulting from DFT calculations.

III. Role of non uniform vertical tunneling

Quantum transport calculations were performed by self-consistently solving the NEGF kinetic equations and the 2D non-linear Poisson equation. Importantly, phonon scattering was considered by adding specific self-energies computed within the self-consistent Born approximation by assuming the deformation potential approximation. The Hamiltonian matrix considered in the NEGF simulations was obtained by discretizing the one in Sec. II.

We are interested in an Esaki tunneling diode made with WSe_2 and $SnSe_2$ and an overlap region of length $L_{\text{OV}} = 6.66\,\mathrm{nm}$, as shown in Fig. 3. WSe_2 and $SnSe_2$ constitute the p-doped source region and the n-doped drain region, respectively, while the vertical tunneling occurs in the overlap region made of the $SnSe_2/WSe_2$ heterostructure.

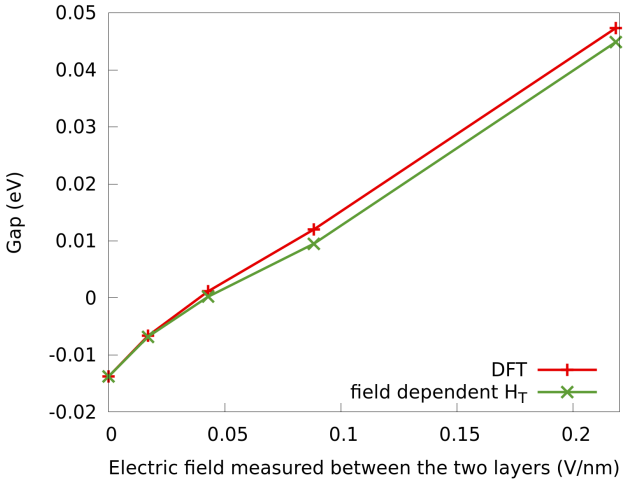

Fig. 2. Band gap of the heterostructure depending on the electric field measured at its centre. The field-dependent curve is computed using the two-band Hamiltonian while the points of the DFT curve are computed *ab initio* for each electric field applied on the gate

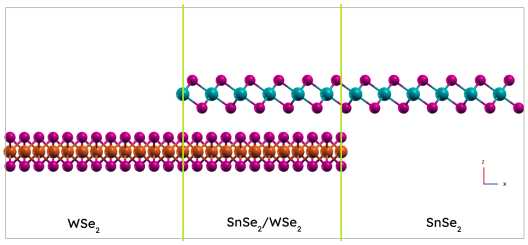

Fig. 3. Illustration of an Esaki diode based on the $SnSe_2/WSe_2$ heterostructure. The length of source and drain regions is 13 nm while the length of the overlap region is L_{OV}. The doping concentration is $-8 \times 10^{13}\,\mathrm{cm}^{-2}$ in the source and $8 \times 10^{13}\,\mathrm{cm}^{-2}$ in the drain.

The I-V characteristics are reported in Fig. 4. To strengthen the importance of considering a non-uniform tunneling coupling in such systems, we compared the curves obtained with the field-dependent $H_T(x)$ in Eq. (2) and a constant H_T as assumed in Ref. [10]. The simulations with constant coupling terms overestimate (underestimate) the current for reverse (forward) voltage bias. This is consistent with the bias dependence of $H_T(x)$ shown in Fig. 5, showing the absolute value of the tunneling coupling as a function of the position in the overlap region and the applied bias. Moreover, with the field-dependent H_T model, we observe that the peak current is shifted to higher voltages compared to the case with constant H_T. The increase of the field-dependent H_T with V, shown Fig. 5, is responsible of this shift as higher H_T results in higher transmission. Hence we obtain a larger current for a higher voltage. Additional analysis comes from Fig. 6, which compares the current spectra obtained with the two models.

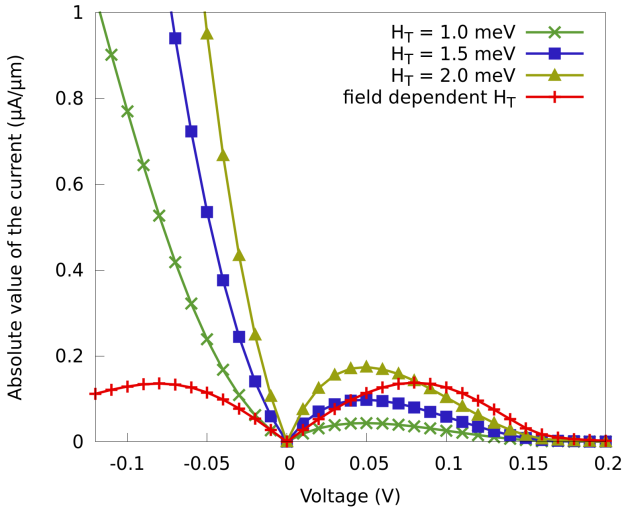

Fig. 4. Current-voltage characteristics of the Esaki diode with an overlap region of length $L_{\mathrm{OV}} = 7\,\mathrm{nm}$ made of the $WSe_2/SnSe_2$ heterostructure. The field-dependent curve was obtained using the expression of H_T given in section II while the others were obtained by replacing this expression by a constant value.

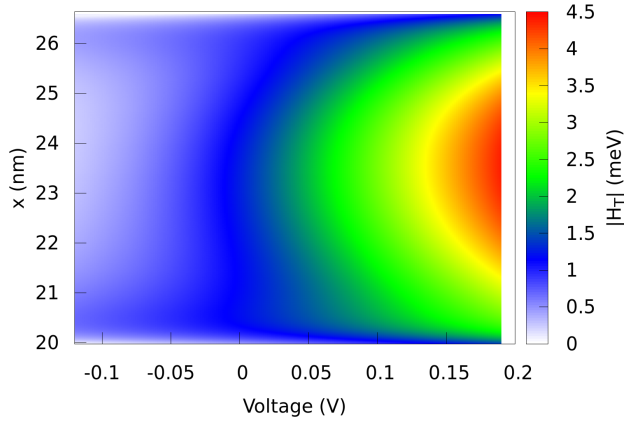

Fig. 5. Colormap of $|H_T|$ as a function of the applied bias and of the x-axis in the overlap region of length $L_{\mathrm{OV}} = 7\,\mathrm{nm}$.

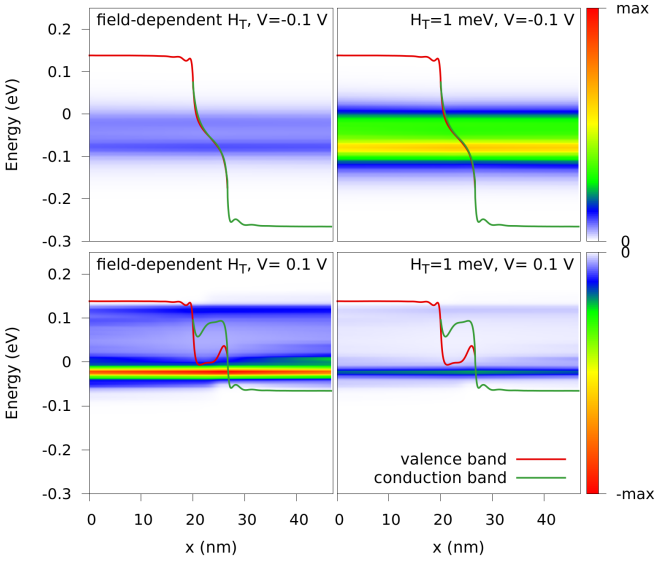

Fig. 6. (Colormap) current spectra along the x-axis for an overlap length of $L_{\mathrm{OV}} = 7\,\mathrm{nm}$. (Left) simulations employing field-dependent H_T; (Right) simulation with constant H_T. The color scale is the same for the two figures on the top and the two on the bottom.

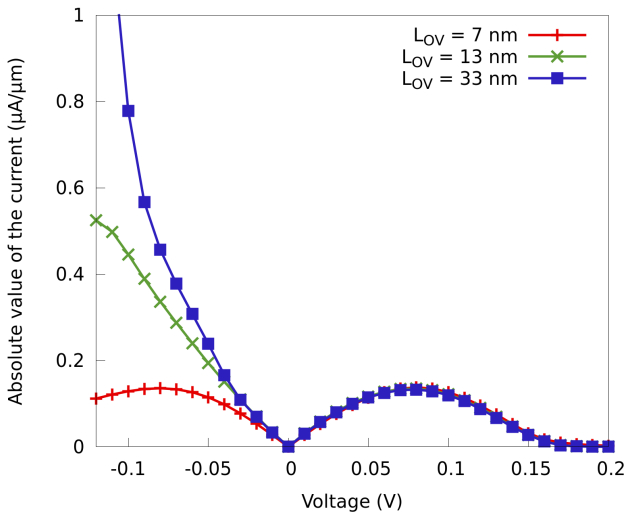

Fig. 7. Current-voltage characteristic of the Esaki diode made with the $WSe_2/SnSe_2$ heterostructure for different lengths of overlap. These were obtained using the field-dependent expression of H_T.

As can be seen, under reverse bias ($V = -0.1\,\mathrm{V}$), the current obtained with the field-dependent coupling is confined to the energy range, where $H_T(x)$ is nonzero (see Fig. 5), whereas in the case of a constant H_T, the current extends over a broader energy range.

Another interesting behaviour that we can notice in the I-V curve (Fig. 4) is that in reverse bias, the current corresponding to the field-dependent $H_T(x)$ tends to decrease for $V < -0.08$ V. This phenomenon is due to the low value of H_T attained at negative voltages, as reported in Fig. 5, thus implying a decrease of the vertical tunneling current.

Finally, we studied the dependence of the current characteristics on the length of the overlap region. To this end, we considered not only $L_{\mathrm{OV}} = 7\,\mathrm{nm}$, but also $L_{\mathrm{OV}} = 13\,\mathrm{nm}$ and $L_{\mathrm{OV}} = 33\,\mathrm{nm}$. In Fig. 7 we report the I-V curves for these three overlap lengths. We notice that the forward bias parts are identical, while in reverse bias the current increases with the overlap. This behaviour can be explained by considering that, in the reverse bias regime, the CB and VB in the middle of the heterostructure are practically inversed. As can be seen in Fig. 8 (top), the vertical tunneling current is therefore non null along all the overlap region, inducing a drain current that increases with L_{OV}. On the contrary, as illustrated in Fig. 8 (bottom), in the forward bias regime the vertical tunneling current between the two materials is mainly located on the edge of the overlap region due to the fact that the CB and VB are separated in the middle of the heterostructure. We have

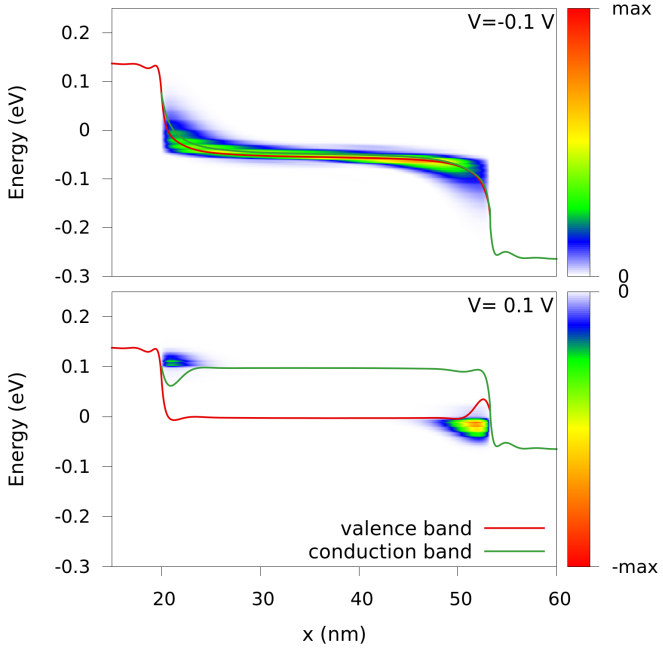

Fig. 8. (Colormap) vertical tunneling current spectra along the x-axis for an overlap of $L_{\mathrm{OV}} = 33\,\mathrm{nm}$ in (top) reverse bias and (bottom) forward bias.

therefore a point-like tunneling device with a drain current almost independent of L_{OV}.

IV. Conclusion

We proposed an efficient model to simulate tunnel devices based on large vdW heterostructures while keeping a complex dependence of tunneling coupling on the vertical electric field validated by DFT. The comparison with the case with constant values of H_T highlights the effects of interlayer coupling on the current, which is highly sensitive to its variations. Our model allowed us to explain the non-trivial dependence of the I-V curves on the geometrical parameters of the Esaki diode based on the $WSe_2/SnSe_2$ vdW heterostructure.

V. Acknowledgments

This work was supported by the French "Agence Nationale de la Recherche" through the projects "Tunne2D" (ANR-21-CE24-0030). D.R. acknowledges support from the HPC resources of IDRIS, CINES, and TGCC under Allocation No. 2024-A0160914101 made by GENCI.

References

[1] S. Fan, Q. A. Vu, S. Lee, T. L. Phan, G. Han, Y.-M. Kim, W. J. Yu, and Y. H. Lee, "Tunable negative differential resistance in van der waals heterostructures at room temperature by tailoring the interface," *ACS Nano*, vol. 13, no. 7, pp. 8193–8201, 2019. [Online]. Available: https://doi.org/10.1021/acsnano.9b03342

[2] B. Zhao, Z. Zhang, J. Xu, D. Guo, T. Gu, G. He, P. Lu, K. He, J. Li, Z. Chen, Q. Ren, L. Miao, J. Lu, Z. Ni, X. Duan, and X. Duan, "Gate-driven band modulation hyperdoping for high-performance p-type 2d semiconductor transistors," *Science*, vol. 388, no. 6752, pp. 1183–1188, 2025. [Online]. Available: https://www.science.org/doi/abs/10.1126/science.adp8444

[3] L. Esaki, "New phenomenon in narrow germanium $p - n$ junctions," *Phys. Rev.*, vol. 109, pp. 603–604, 01 1958. [Online]. Available: https://link.aps.org/doi/10.1103/PhysRev.109.603

[4] P. Giannozzi, O. Andreussi, T. Brumme, O. Bunau, M. Buongiorno Nardelli, M. Calandra, R. Car, C. Cavazzoni, D. Ceresoli, M. Cococcioni, N. Colonna, I. Carnimeo, A. Dal Corso, S. de Gironcoli, P. Delugas, R. A. DiStasio, A. Ferretti, A. Floris, G. Fratesi, G. Fugallo, R. Gebauer, U. Gerstmann, F. Giustino, T. Gorni, J. Jia, M. Kawamura, H.-Y. Ko, A. Kokalj, E. Küçükbenli, M. Lazzeri, M. Marsili, N. Marzari, F. Mauri, N. L. Nguyen, H.-V. Nguyen, A. Otero-de-la Roza, L. Paulatto, S. Poncé, D. Rocca, R. Sabatini, B. Santra, M. Schlipf, A. P. Seitsonen, A. Smogunov, I. Timrov, T. Thonhauser, P. Umari, N. Vast, X. Wu, and S. Baroni, "Advanced capabilities for materials modelling with quantum ESPRESSO," *Journal of Physics: Condensed Matter*, vol. 29, no. 46, p. 465901, 11 2017. [Online]. Available: https://iopscience.iop.org/article/10.1088/1361-648X/aa8f79

[5] J. P. Perdew, K. Burke, and M. Ernzerhof, "Generalized gradient approximation made simple," *Phys. Rev. Lett.*, vol. 77, pp. 3865–3868, 10 1996. [Online]. Available: https://link.aps.org/doi/10.1103/PhysRevLett.77.3865

[6] S. Grimme, J. Antony, S. Ehrlich, and H. Krieg, "A consistent and accurate ab initio parametrization of density functional dispersion correction (dft-d) for the 94 elements h-pu," *The Journal of Chemical Physics*, vol. 132, no. 15, p. 154104, 04 2010. [Online]. Available: https://doi.org/10.1063/1.3382344

[7] O. Morandi and M. Modugno, "Multiband envelope function model for quantum transport in a tunneling diode," *Phys. Rev. B*, vol. 71, p. 235331, 06 2005. [Online]. Available: https://link.aps.org/doi/10.1103/PhysRevB.71.235331

[8] J. Cao, D. Logoteta, M. G. Pala, and A. Cresti, "Impact of momentum mismatch on 2d van der waals tunnel field-effect transistors," *Journal of Physics D: Applied Physics*, vol. 51, no. 5, p. 055102, 2018.

[9] T. Sohier, M. Calandra, and F. Mauri, "Density functional perturbation theory for gated two-dimensional heterostructures: Theoretical developments and application to flexural phonons in graphene," *Phys. Rev. B*, vol. 96, p. 075448, 08 2017. [Online]. Available: https://link.aps.org/doi/10.1103/PhysRevB.96.075448

[10] J. Cao, D. Logoteta, S. Özkaya, B. Biel, A. Cresti, M. G. Pala, and D. Esseni, "Operation and design of van der waals tunnel transistors: A 3-d quantum transport study," *IEEE Transactions on Electron Devices*, vol. 63, no. 11, pp. 4388–4394, 2016.